J-Researchers

Journal of Civil Engineering Researchers

Journal homepage: www.journals-researchers.com

Optimal Placement of Viscoelastic Layers in Sandwich Beams for Maximum Vibration Attenuation and Minimum Creep Deflections

A.R. Gorji, [a] M. Lezgy-Nazargah, [a,*] A. Ghafourian-Mojaver, [a] M. Tayebinia [a]

[a] *Department of Civil Engineering, Faculty of Engineering, Hakim Sabzevari University, Sabzevar 9617976487-397, Iran*

ABSTRACT

Until now, various mathematical models have been proposed to characterize the behavior of viscoelastic materials and facilitate their implementation in finite element software. However, it remains unclear which configuration of the viscoelastic layer along the thickness and length of the beam yields the lowest creep deflection and highest damping effect under applied forces. To fill this literature gap, efforts are undertaken in this study to identify the optimal placement of the viscoelastic layers in the sandwich beam. To reach this aim, the creep and dynamic behaviors of sandwich beams with different boundary conditions and various configurations of the viscoelastic layer along the thickness and length were investigated using a finite element model. The obtained results indicate that the damping capability and creep deformations of the sandwich beam are strongly affected by the position of the viscoelastic layers.

ARTICLE INFO

Received: June 30, 2025
Accepted: September 08, 2025

Keywords:
Sandwich beams
Viscoelastic layers
Vibration attenuation
Optimal position
Finite element

DOI: 10.61186/JCER.7.4.78
DOR: 20.1001.1.22516530.1399.11.4.1.1

1. Introduction

In recent years, the application of viscoelastic materials has increased significantly. The growing interest in these materials arises from their ability to dissipate significant amounts of energy through shear deformation. These materials are predominantly utilized as energy dampers. On the other hand, sandwich structures are widely utilized in industries such as construction, bridge building, and shipbuilding, owing to their high bending stiffness-to-weight ratio and the adaptability to modify fundamental structural parameters to meet specific design requirements. Sandwich beams with viscoelastic cores, known for their effective damping properties under dynamic loads, are among the most widely used components in industrial structures.

Banks et al. [1] provided a comprehensive overview of elastic and viscoelastic materials, aiming to enhance the understanding of their properties and applications. Lakes [2] conducted experimental studies to explore the properties of viscoelastic materials across a range of substances, including polymers, metals, piezoelectric materials, damping alloys, composites, and biological materials. Galuppi and Royer-Carfagni [3] analyzed the time-dependent behavior of a sandwich beam with viscoelastic core. The analyzed beam comprises two elastic layers at the top and bottom, with a viscoelastic core sandwiched between them. Galuppi and Roier-Carfagni

* Corresponding author. Tel.: +980000000000; e-mail: m.lezgy@hsu.ac.ir.

compared the results obtained from their analytical model with those obtained from three-dimensional finite element analysis. Kpeky et al. [4] investigated the vibration behavior of sandwich structures featuring soft and flexible cores. Given the substantial differences in the mechanical properties between the core and the top and bottom layers of sandwich structures, modeling these systems using higher-order elements or three-dimensional elements is more suitable. However, this approach increases the number of degrees of freedom and extends the analysis time. To mitigate this time-consuming process, Kpeky and colleagues proposed a hexahedral solid-shell linear element as an alternative.

Mohammadi and Nasirshoaibi [5] detailed the modeling process for viscoelastic materials using ABAQUS software. This reference emphasizes that the behavior of viscoelastic materials can be effectively simulated by precisely defining the storage and loss shear moduli. The simulation results were then compared with experimental data. Pelayo et al. [6] investigated the temperature- and time-dependent behavior of polyvinylbutyral (PVB) material, commonly used in the construction of sandwich beams. This reference examines the mechanical behavior of laminated glass elements in which PVB, a viscoelastic material, is used as an interlayer. In this research, PVB samples were subjected to dynamic tests using a dynamic mechanical thermal analysis (DMTA) device across a temperature range of -15°C to 50°C. Subsequently, master curves at different temperatures were constructed using the Williams-Landel-Ferry model, and the Young's modulus of PVB was determined in both time and frequency domains.

Froli and Lani [7] investigated the adhesion, creep, and stress relaxation behavior of laminated glass incorporating a viscoelastic PVB interlayer. In this reference, glass specimens were subjected to tensile loading at a 45-degree angle relative to their longitudinal axis. A modified shear-compression testing method was utilized to assess evaluate the ultimate shear strength of the PVB interlayers. Various specimens of this material were fabricated and experimentally tested. Following the experimental investigations, the viscoelastic properties of the material, specifically shear behavior, creep, and stress relaxation, were characterized and subsequently used in numerical modeling. Ehrich et al. [8] proposed a new methodology for examining the properties of encapsulated ethylene-vinyl acetate (EVA) and PVB. The newly developed method for characterizing encapsulated materials demonstrated high effectiveness, cost-efficiency, and practicality for laboratory-scale applications. Hána et al. [9] conducted both experimental and numerical studies to evaluate the mechanical properties of polymer interlayers used in laminated glass manufacturing. These researchers investigated the sensitivity of shear stiffness in two commonly used polymers in glass panel construction—PVB and EVA—to variations in time and temperature. Hána et al. [10] investigated the four-point bending behavior of glass panels with PVB interlayers using both numerical and experimental approaches. The analyzed glass panels were composed of glass sheets bonded by polymer interlayers, which enabled the transfer of shear stresses between the glass layers. Hána, Eliášová and colleagues determined the time- and temperature-dependent shear stiffness using a discrete Maxwell model, with Prony series coefficients derived from the thermo-dynamic analysis of the polymer interlayer.

Zemanová et al. [11] analyzed the modal characteristics of multilayered glass beams. Given that in laminated glass, rigid glass layers are bonded with soft interlayers whose mechanical behavior is frequency and temperature-dependent, the system exhibits viscoelastic characteristics. In this reference, Zimanová et al. employed four distinct approaches to address to solve the nonlinear eigenvalue problem: complex eigenvalue computation based on the Newton-Raphson method, the modal kinetic energy method, the dynamic effective thickness method, and the enhanced effective thickness method. Li et al. [12] presented a state-space method for analyzing the dynamic response of double-layer beams with a viscoelastic interlayer. The considered double-layer system consists of two parallel Euler-Bernoulli elastic beams connected by a generalized viscoelastic interlayer. In this reference, a novel state-space approach is developed by introducing mode shape constants to address the coupling effects induced by the viscoelastic interlayer. Schuster et al. [13] investigated the linear viscoelastic behavior of polymeric interlayers used in laminated glass. This study examined a three-layer system consisting of rigid outer layers and a soft acoustic PVB core, emphasizing the impact of temperature and loading on the materials mechanical properties. The experimental data analysis included DMTA and creep testing under bending conditions. In this reference, the results were compared with analytical models developed using the generalized Maxwell model and a simplified model that combined multiple rheological models.

Based on the studies conducted so far, it can be concluded that accurately predicting the dynamic behavior of sandwich beams with viscoelastic layers using the finite element method necessitates a precise determination of the structural properties and constitutive relationships of viscoelastic materials. Various methods are available to define the characteristics of viscoelastic materials, including the utilization of dynamic storage and loss moduli, creep or relaxation test data, or directly specifying of Prony series parameters. However, no comprehensive study has been conducted to date to determine the optimal placement of the viscoelastic layer. This research seeks to determine the optimal positioning of viscoelastic layers

along the thickness and length of the beam to maximize damping performance.

2. Sandwich beam with viscoelastic layers

2.1. Geometry and mechanical properties

The considered sandwich beams of the present study are prismatic, featuring a rectangular uniform cross-section of width b, height h, and length L. These sandwich beams comprising three glass layers and two viscoelastic layers made of PVB material. The total thickness of glass layers is $3h_G$, while the total thickness of PVB layers is $2h_V$. Laminated glass beams are widely used in diverse structural applications. They form the primary support ribs or secondary purlins for large overhead glazed roofs, entrance canopies, and atria. They also serve as load-bearing elements for glass floors, bridges, and stair stringers/treads where transparency is desired for visual connection or light penetration. Since the failure of glass structures is rather brittle, PVB laminates are incorporated as safety-critical enhancements. The PVB layers provide essential post-breakage integrity. If a laminated glass beam is impacted (e.g., by hail, falling debris), the PVB holds shattered glass fragments in place, preventing collapse and protecting people below. Additionally, PVB laminates enhance vibration damping.

To identify the optimal position of the viscoelastic layers along the beam's thickness, four distinct lay-up schemes are assumed for the sandwich beams. These considered lay-up schemes are illustrated in Fig. 1. Notably, in all these lay-up schemes, the total cross-sectional area of the viscoelastic layers remains identical.

In this paper, the optimal placement of viscoelastic layers along the beam's longitudinal axis is also investigated. For this purpose, various configurations for positioning the PVB layer along the beam's length are considered. As illustrated in Fig. 2, the three considered axial configurations for the placement of the PVB layer along the beam length are:

- The first third of the beam,
- The middle third of the beam,

The last third of the beam.

2.2. Constitutive relations for viscoelastic materials

This section focuses on the constitutive equations of linear viscoelastic materials and their corresponding linear constitutive relations. Linear viscoelasticity is generally applicable only to small deformations or to materials that exhibit linear mechanical behavior.

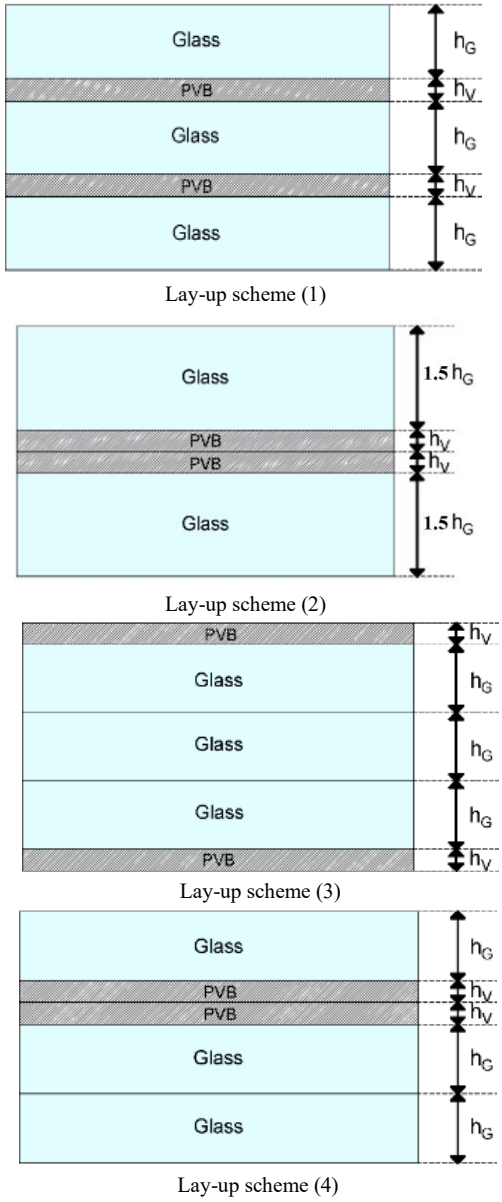

Fig. 1 Different lay-up schemes considered for the sandwich beams

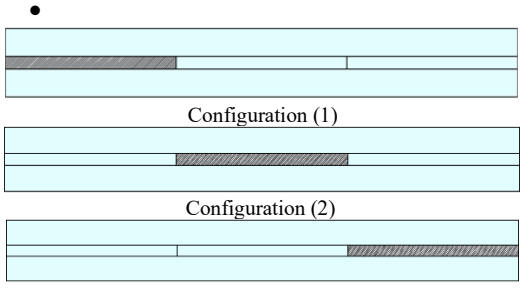

Fig. 2. Different configurations for the placement of the viscoelastic layers along the beam's longitudinal axis

Therefore, the theory of infinitesimal strains is typically employed in the analysis of such materials. One of the most widely used and general approaches for modeling linear viscoelastic materials is the Boltzmann superposition principle, originally introduced by Ludwig Boltzmann Lakes [2]. The Boltzmann Superposition Principle asserts that the total response of a system is equal to the sum of the individual responses caused by each component acting independently. To predict the stress history in viscoelastic materials, it is assumed that a specific strain is applied to the material. Relaxation and recovery experiments are commonly conducted to verify the linearity of this principle, ensuring that the material's response adheres to the principle under the applied conditions. The time-dependent relaxation stress is expressed as:

$$\sigma_0 = \varepsilon_0 E(t) \tag{1}$$

where ε_0 represents the initial strain, and $E(t)$ is the relaxation modulus. Based on the Boltzmann Superposition Principle, an arbitrary strain history can be represented as a combination of two sequential unit step strains:

$$\varepsilon(t) = \varepsilon_0[H(t) - H(t - t_1)] \tag{2}$$

where $H(t)$ denotes the Heaviside step function. Thus, as described in Fig. 3, the resulting stress is:

$$\sigma(t) = \varepsilon_0[E(t) - E(t - t_1)] \tag{3}$$

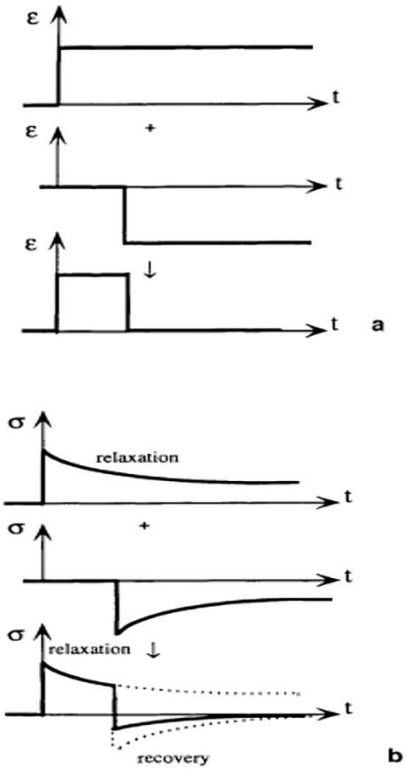

Fig. 3. (a) Application of the Boltzmann Superposition Principle to generate a strain pulse, (b) Calculation of relaxation stress in response to a strain pulse using the Boltzmann Superposition Principle

The stress resulting from the delayed strain $\varepsilon_0 H(t - t_1)$ is expressed as $\varepsilon_0 E(t - t_1)$, similar to the stress $\varepsilon_0 E(t)$, generated by the preceding strain step $\varepsilon_0 H(t)$. This relationship holds under the assumption that the material properties remain constant over time. Depending on the material's viscoelastic characteristics, the stress may diminish to zero or recover as time t progresses Lakes [2]. The strain history $\varepsilon(t)$ is defined as a function of time t, as depicted in Fig. 4. It is assumed that the strain remains zero before $t = 0$. A specific segment of this strain history, ranging from $t - \tau$ to $t - \tau + \Delta\tau$ (where τ is a time variable, analogous to the constant t_1 in the earlier equations), is illustrated in Fig. 4. This segment of the strain history can be mathematically represented as:

$$\varepsilon(t) = \varepsilon(\tau)[H(t - \tau) - H(t - \tau + \Delta\tau)] \tag{4}$$

The equation above effectively describes a strain pulse.

Using Eq. (3), the variation in stress within the viscoelastic material resulting from the strain pulse history can be formulated as:

$$d\sigma(t) = \varepsilon(\tau)[E(t - \tau) - E(t - \tau + \Delta\tau)] \tag{5}$$

On the other hand, we have:

$$\frac{dE(t-\tau)}{d\tau} = \lim_{\Delta t \to 0} \frac{E(t - \tau + \Delta\tau) - E(t - \tau)}{\Delta\tau} \tag{6}$$

Thus, the stress increment can be written as:

$$d\sigma(t) = -\varepsilon(t)\frac{dE(t-\tau)}{d\tau} \tag{7}$$

The entire strain history can be broken down into discrete strain pulses. The stress at any given time t is determined by summing the stress contributions from all preceding pulses. Importantly, only the effects of strain pulses that occur before the present time t are included in the computation. Contributions from potential future strain pulses are not accounted for, ensuring causality in the stress-strain relationship.

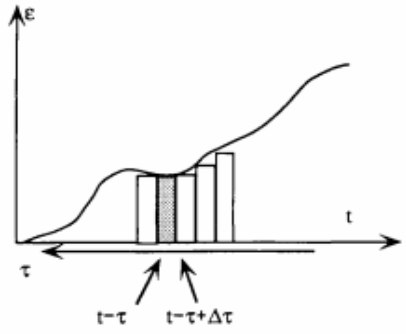

Fig. 4. Decomposition of the strain history into a series of strain pulses

If the width of the strain pulses, denoted as $\Delta\tau$ approaches an infinitesimally small value, the summation converges to an integral, yielding the following expression for stress:

$$\sigma(t) = -\int_0^t \varepsilon(\tau)\frac{dE(t-\tau)}{d\tau}d\tau + E(0)\varepsilon(t) \tag{8}$$

The second term in this equation arises due to the following rationale: After the strain pulse or a series of

strain pulses, the strain often returns to zero. However, for an arbitrary strain history, the final strain, $\varepsilon(t)$, at time t is generally nonzero. The stress increment associated with the final strain is given by $E(0)\varepsilon(t)$, as there is insufficient time for stress relaxation to occur in this scenario Lakes [2]. To derive the final form of Boltzmann's superposition principle, integration by parts is applied. In this formulation, t represents time, and τ represents the time variable for integration:

$$\sigma(t) = \int_0^t E(t-\tau)\frac{d\varepsilon(\tau)}{d\tau}d\tau \tag{9}$$

If the roles of stress and strain in the preceding discussions are interchanged, the complementary relationship below is obtained:

$$\varepsilon(t) = \int_0^t J_E(t-\tau)\frac{d\sigma(\tau)}{d\tau}d\tau \tag{10}$$

Consequently, if the response of a viscoelastic material to a unit step stress or strain is experimentally measured, the material's behavior under any arbitrary load history can be computed.

The effect of temperature θ on the behavior of a viscoelastic material can be explained by using the concept of reduced time. In this case, the stress-strain relation is rewritten as:

$$\sigma(t) = E_0(\theta)\gamma - \int_0^t \dot{E}\big(\xi(s)\big)\varepsilon(t-s)ds \tag{11}$$

where $\dot{E}(\xi) = \frac{dE}{d\xi}$. In addition, $\xi(t)$ is the reduced time defined as:

$$\xi(t) = \int_0^t \frac{ds}{\alpha(\theta(s))} \tag{12}$$

In the above equation, $\alpha(\theta(s))$ is time transmission function defined as:

$$\log(\alpha) = -\frac{C_1(\theta-\theta_0)}{C_2+(\theta-\theta_0)} \tag{13}$$

where θ_0 is the reference temperature at which the viscoelastic material response is measured. C_1 and C_2 are the calibration constants measured at this temperature.

The previous paragraphs examined the constitutive relations in a one-dimensional state. For a viscoelastic material in three dimensions, the constitutive relationship can be expressed in the following form:

$$\sigma_{ij}(t) = \int_0^t C_{ijkl}(t-\tau)\frac{d\varepsilon_{kl}(\tau)}{d\tau}d\tau \tag{14}$$

where C_{ijkl} denotes elastic constants of a viscoelastic material. The above equation can be rewritten as the following matrix form:

$$\boldsymbol{\sigma}(t) = \boldsymbol{C}(t)\boldsymbol{\varepsilon}(t) \tag{15}$$

2.3. Finite element modeling

The finite element model employed to analyze the viscoelastic sandwich beam utilizes an 8-node continuum solid element. Each node has three degrees of freedom corresponding to translations along the global coordinate axes of x_1, x_2, and x_3. The vector of displacement components $\boldsymbol{u} = [u \quad v \quad w]^T$ may be written in terms of the nodal variables vectors $\boldsymbol{u}_u^e$ as follows:

$$u = N_{uu}u_u^e \tag{16}$$

where

$$\boldsymbol{u}_u^e = \{u_1 \quad u_2 \quad \cdots \quad u_8 \quad \vdots \quad v_1 \quad v_2 \quad \cdots \quad v_8 \quad \vdots \quad w_1 \quad w_2 \quad \cdots \quad w_8\}^T$$

In Eq. (16), $\boldsymbol{N}_{uu}$ denotes displacements Lagrange interpolation matrix. For brevity, the expression for $\boldsymbol{N}_{uu}$ is not included here.

The Strain components at any point within the viscoelastic beam can be expressed in the following matrix form:

$$\boldsymbol{\varepsilon} = \boldsymbol{L}_{uu}\boldsymbol{u} \tag{17}$$

where

$$\boldsymbol{L}_{uu} = \begin{bmatrix} \partial/\partial x & 0 & 0 \\ 0 & \partial/\partial y & 0 \\ 0 & 0 & \partial/\partial z \\ 0 & \partial/\partial z & \partial/\partial y \\ \partial/\partial z & 0 & \partial/\partial x \\ \partial/\partial y & \partial/\partial x & 0 \end{bmatrix}$$

$$\boldsymbol{\varepsilon} = [\varepsilon_{11} \quad \varepsilon_{22} \quad \varepsilon_{33} \quad 2\varepsilon_{23} \quad 2\varepsilon_{13} \quad 2\varepsilon_{12}]^T$$

Given that the displacement components of the sandwich beam with viscoelastic layers are small, the linear strain-displacement relationships are utilized in Eq. (6). For a 8-node continum finite element with three degrees of freedom per node, and by using Eq. (16), strain vector may be expressed as follows:

$$\boldsymbol{\varepsilon} = \boldsymbol{L}_{uu}\boldsymbol{u} = \boldsymbol{L}_{uu}\boldsymbol{N}_{uu}\boldsymbol{u}_u^e = \boldsymbol{B}\boldsymbol{u}_u^e \tag{18}$$

where $\boldsymbol{B}$ denotes strain interpolation matrix.

The Hamilton's principle is used to derive governing equations of the viscoelastic sandwich beam. According to this principle, for a viscoelastic medium with volume Ω and regular boundary surface Γ, The following relationship applies:

$$\delta\left[\int_0^t (U_0 - T_k)dt\right] = 0 \tag{19}$$

where

$$U_0 = \frac{1}{2}\int_\Omega \boldsymbol{\varepsilon}^T\boldsymbol{\sigma}d\Omega - \int_\Gamma \boldsymbol{u}^T\boldsymbol{F}_S d\Gamma - \int_\Omega \boldsymbol{u}^T\boldsymbol{F}_V d\Omega \tag{20}$$

$$T_k = \frac{1}{2}\int_V \rho\frac{\partial\boldsymbol{u}^T}{\partial t}\frac{\partial\boldsymbol{u}}{\partial t}dV, \tag{21}$$

and ρ is the density. In addition, $\boldsymbol{F}_S$ and $\boldsymbol{F}_V$ are surface force vector, respectively. Substituting Eqs. (15), (16), and (18) into Eq. (19), and assembling the element equations result in the following general equation:

$$\boldsymbol{M}\ddot{\boldsymbol{q}}(t) + \boldsymbol{K}(t)\boldsymbol{q}(t) = \boldsymbol{F}(t) \tag{22}$$

The matrices and vectors in the above equation include the stiffness matrix $\boldsymbol{K}(t) = \int_\Omega \boldsymbol{B}^T\boldsymbol{C}\boldsymbol{B}d\Omega$, mass matrix $\boldsymbol{M} = \int_\Omega \rho\mathbf{N}_{uu}^T\boldsymbol{N}_{uu}d\Omega$, and loads vector $\boldsymbol{F}(t) = \int_\Omega \boldsymbol{N}_{uu}{}^T\boldsymbol{F}_V d\Omega + \int_\Gamma \boldsymbol{N}_{uu}{}^T\boldsymbol{F}_S d\Gamma$.

3. Numerical Results and Discussion

In this section, numerical examples are presented to investigate the influence of viscoelastic layers' position on the natural frequency, damping capability, and creep deformations of sandwich beams. Firstly, the finite element model is validated by comparing its results with experimental data. Then, the optimal placement of viscoelastic layers within sandwich beams is determined.

All sandwich beams examined in this section have a length of 1000 mm, a width of 100 mm, and their overall thickness is 12.76 mm. The thickness of each glass layer is 4 mm, while the thickness of each viscoelastic layer is 0.38 mm. The layers are assumed to be perfectly bonded, ensuring no slippage at the interfaces. The mechanical properties of the glass and the viscoelastic material (i.e., PVB) are summarized in Table 1. Thermal effects are neglected, and the analyses are performed at the constant temperature of 20°C.

All numerical simulations are carried out using ABAQUS software. The eight-node brick element (C3D8R) available in the library of this software was employed for modeling the glass and PVB layers. Static analysis was adopted for simulating the creep problems. Dynamic implicit analysis was used for predicting the transient creep responses. Free vibration tests were also carried out by employing the eigenvalue solver available in the ABAQUS software.

Table 1
Mechanical Properties of Glass and PVB [6]

Material	Elastic Modulus (MPa)	Poisson's Ratio	Density (kg/m³)	C_1	C_2
Glass	72000	0.22	2,500	12.6010	74.76
PVB	1240.3	0.49	1100	12.6010	74.76

3.1. Validating example

Free vibration analysis of a sandwich beam with viscoelastic layers is studied in this subsection. The sandwich beam under consideration has clamped boundary conditions at both ends.. Lamination configuration of the sandwich beam is lay-up 1 (see Fig. 1). The viscoelastic layers are located all over the length of the beam. This analysis aims to assess and compare the accuracy of the 3D finite element simulations. Experimental data from Pelayo et al. [6], who previously studied this beam, are employed to validate the numerical results.

Table 2 summarizes the first four natural frequencies of the viscoelastic sandwich beam, calculated using the finite element model. The numerical results are compared with the experimental data reported by Pelayo et al. [6].

Table 2
Natural Frequencies (Hz) of the clamped-clamped sandwich beam with lay-up scheme no. 1

Vibrating Mode	Experimental	Present
1	36.14	36.47
2	98.28	97.40
3	188.94	188.22
4	306.13	303.35

Table 2 demonstrates that the numerical results from the finite element model align exceptionally well with the experimental data, showing a maximum percentage discrepancy of just 0.9%.

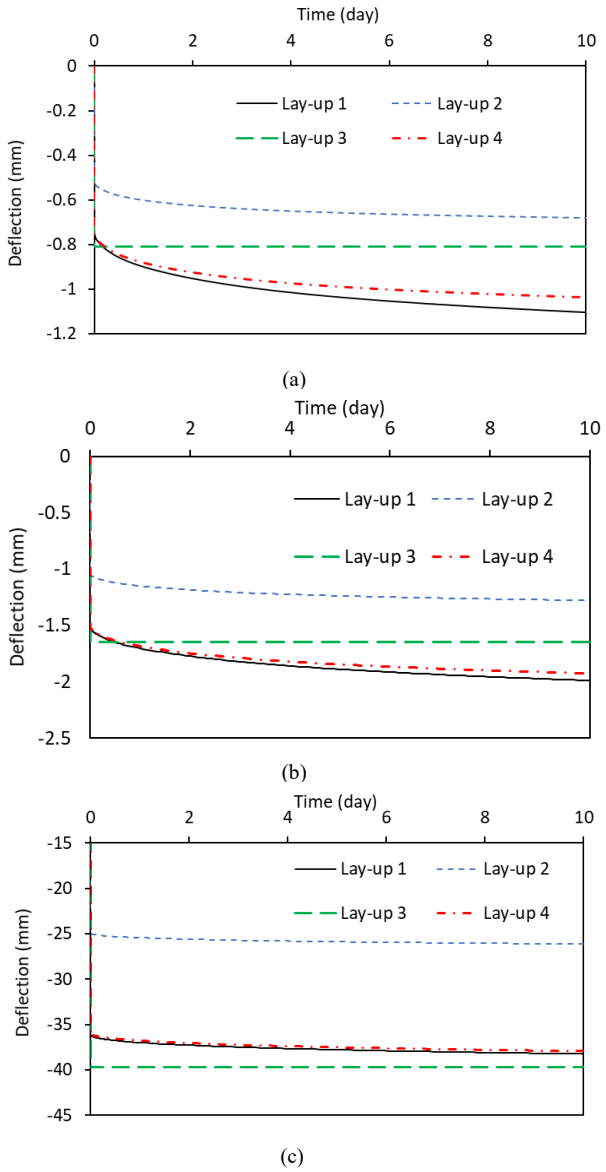

Fig. 5. Effect of lay-up scheme on the long-term deflection of sandwich beams: (a) clamped-clamped, (b) simply support, (c) clamped-free

Table 4
Effect of lamination configuration on the natural frequencies (Hz) of the sandwich beams

Boundary condition	Mode no.	Laminaion configuration			
		Lay-up 1	Lay-up 2	Lay-up 3	Lay-up 4
Fixed-Fixed	1	36.472	52.195	51.463	40.587
	2	97.402	142.44	141.72	110.13
	3	188.22	277.84	277.89	214.49
	4	303.35	312.00	372.07	351.18
Simply support	1	18.09	24.02	22.22	18.95
	2	64.43	92.09	88.99	70.99
	3	139.96	204.85	200.67	157.22
	4	245.21	257.67	257.67	257.67
Clamped-free	1	7.2641	9.1232	7.9996	7.4169
	2	37.688	52.293	50.076	40.871
	3	59.945	59.945	59.950	59.946
	4	99.072	143.06	140.19	110.49

3.2. Effect of PVB stacking sequence on natural frequency, creep deformations, and damping capability

This section investigates how the through-thickness positioning of viscoelastic layers affects the long-term creep deformations, natural frequencies, and damping capability of the sandwich beams. In the examined sandwich beams of this section, it is assumed that the viscoelastic layers are located all over the length of the structure (configuration 4).

3.2.1. Creep deformations.

The creep deformations of the beam under a uniform load of $2000\ N/m^2$ were calculated for four different lay-up schemes shown in Fig. 1 over a ten-day period. Variations of maximum deflection with respect to time are shown in Figs. 5a, 5b, and 5c. Moreover, the percentage increase in the beam's creep deformation during this time frame is summarized in Table 3.The analysis reveals that, irrespective of the boundary conditions, the third lay-up scheme leads to the minimum rate of time-dependent deflections. For instance, in a cantilever sandwich beam, the percentage increase in deformations for lay-up scheme 1, through 4 are 5.99%, 4.87%, 0.59%, and 5.41%, respectively. The corresponding increases in deformation for other boundary conditions are summarized in Table 3.

Table 3
Percentage increase (%) in the long-term deflection of the sandwich beam for different lay-up schemes

Boundary Conditions	Lay-up 1	Lay-up 2	Lay-up 3	Lay-up 4
Clamped-Free	5.99%	4.87%	0.59%	5.41%
Clamped-Clamped	33.48%	24.70%	0.59%	29.36%
Simply supported	24.92%	19.13%	0.59%	25.59%

3.2.2. Natural frequencies.

Table 4 shows the first four natural frequencies of sandwich beams for different lay-up schemes and various boundary conditions. It is seen that the natural frequencies are very sensitive with respect to the lay-up scheme chosen for the sandwich beam. Regardless of the type of boundary conditions, lay-up scheme 2 leads to the highest frequency, and lay-up scheme 1 leads to the lowest frequency among other lamination configurations.

As observed in Figs. 8-10, the second viscoelastic layer configuration provides superior damping performance under different boundary conditions, leading to faster dissipation of beam vibrations. For example, for a sandwich beam with a clamped-free boundary condition, vibrations are reduced by more than 99% within 3.96 seconds when using the second configuration. In contrast, the corresponding reduction times for the first, third, and fourth lamination configurations are 4.29, 4.32, and 4.68 seconds, respectively. The results for other boundary conditions are summarized in Table 5.

Table 5.
Effect of different lamination configurations on the vibration decay time

Boundary Conditions	Lay-up 1	Lay-up 2	Lay-up 3	Lay-up 4
Clamped-Free	4.29 s	3.96 s	4.32 s	4.68 s
Clamped-Clamped	2.67 s	2.12 s	2.78 s	2.74 s
Simply supported	2.15 s	1.70 s	2.56 s	2.39 s

3.2.3. Damping capability

The influence of the lay-up configuration on the reduction of dynamic vibrations and the damping behavior of sandwich beams is investigated in this subsection. For the four distinct lay-up schemes shown in Fig. 1, the time history of the beams' maximum deflection is estimated using the finite element simulation. It is worth noting that the analyzed sandwich beams were initially subjected to a predefined initial deformation and subsequently released. The analyzed sandwich beams are assumed to have three different boundary conditions: clamped-free, simply supported, and clamped-clamped. The deflection time-history of sandwich beams with different boundary conditions are shown in Figs. 6a, 6b, and 6c.

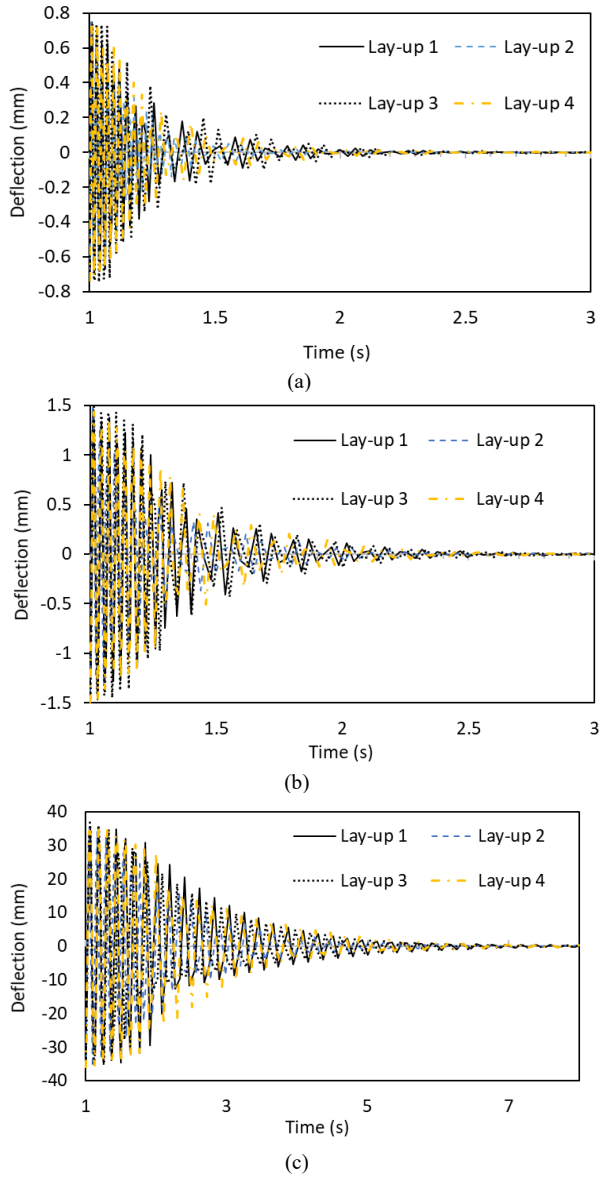

Fig. 6. Effect of lay-up configuration on the time-history response of sandwich beams: (a) clamped-clamped, (b) simply support, (c) clamped-free

3.3. Effect of axial location of PVB layers on creep deformations and damping capability

In the previous section, the optimal placement of the viscoelastic layers across the beam's thickness was investigated. The results indicated that, regardless of the boundary conditions, placing the viscoelastic layers at the central part of the beam's thickness (i.e., lay-up scheme 2) provides the highest damping efficiency. In this section, the effects of axial location of PVB layers on creep deformations and damping capabilities are investigated. Based on the results of Section 3.2, the lamination configuration of all examined sandwich beams of this section is lay-up no. 2 (see Fig. 1).

3.3.1. Creep deformations

For three different configurations of PVB layer placement, the creep deformation of the beam under a uniform distributed load of 2000 N/m^2 was evaluated after ten days. The results are illustrated in Figs. 7a, 7b, and 7c. Moreover, the percentage increase in the beam's creep deformation during this time frame is summarized in Table 6.

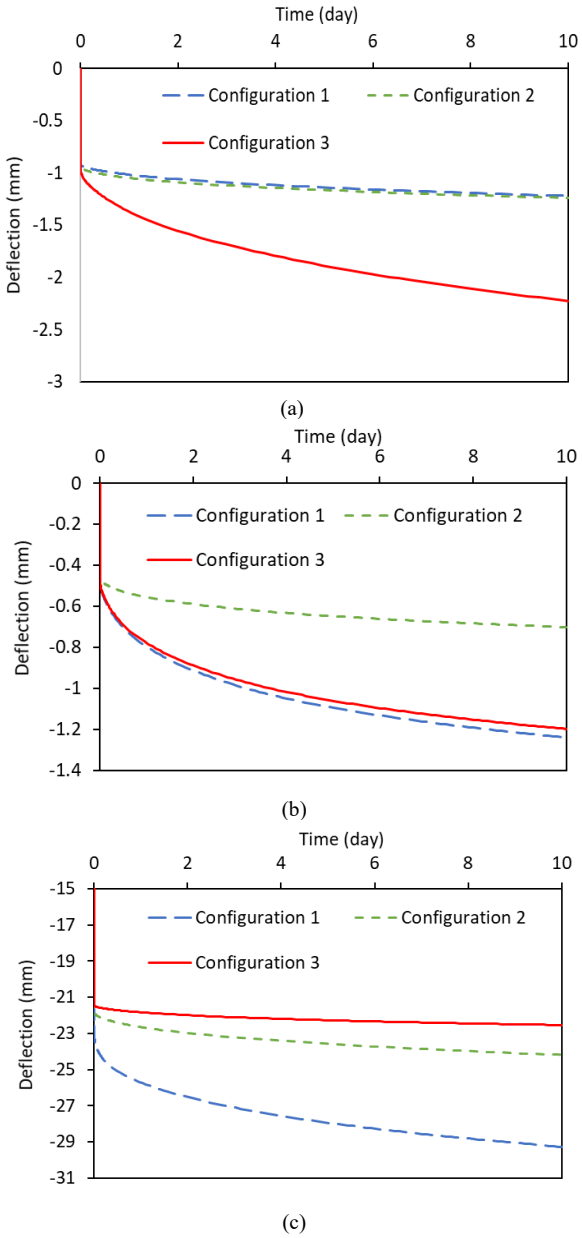

Fig. 7 Effect of the longitudinal position of the PVB layer on the maximum creep deformation of sandwich beam: (a) simply support, (b) clamped-clamped, (c) clamped-free

Table 6.
Percentage increase (%) in long-term deflection of the sandwich beam for different longitudinal positions of the PVB layers

Boundary Conditions	Configuration 1	Configuration 2	Configuration 3
Clamped-Free	25.04	14.60	4.94
Clamped-Clamped	63.86	36.52	63.86
Simply support	33.17	66.86	33.17

Table 6 shows that for simply supported and clamped-clamped sandwich beams, placing the PVB layer within the middle third of the beam's length minimizes the rate of time-dependent creep deflections. In contrast, for clamped-free sandwich beams, the minimum rate of creep deformations occurs when the PVB layer is located in the last third of the beam.

3.3.2. Damping capability

For three different axial locations of the PVB layers shown in Fig. 2, the time-history of the maximum deflection of the beams are estimated using the finite element simulation. The analyzed sandwich beams were subjected to an initial deformation, with various boundary conditions assumed, including clamped-free, simply supported, and clamped-clamped, are assumed for them.

Fig. 8a shows the deflection time history of sandwich beams with clamped-free end conditions. As shown in Figure 19, placing the PVB layer near the free end of the cantilever beam leads to a faster attenuation of transverse vibrations compared to other configurations. The beam vibration amplitude are reduced by more than 99% after 5.82, 5.74, and 5.71 seconds for configurations 1, 2, and 3, respectively. Although the differences in decay times are minor, the results highlight that the damping performance is sensitive to the longitudinal position of the viscoelastic interlayer, with improved performance observed when the layer is placed closer to the free end.

Fig. 8b illustrates the dynamic response of a clamped-clamped sandwich beam under different longitudinal configurations of the PVB layer. Compared to the cantilever beams, the clamped-clamped sandwich beams show significantly faster vibration decay due to increased global stiffness. The vibrations are nearly damped out within 0.4 seconds in all cases. Although differences between the three configurations are minimal, the highest damping is achieved when the PVB layer is positioned in the middle third of the beam.

Fig. 8c shows the deflection time history of a simply supported sandwich beam under different longitudinal configurations of the PVB layer. All configurations demonstrate rapid vibration decay, with displacements significantly reduced within approximately 2.5 seconds. Among the three configurations, configuration 3 (red curve) slightly outperforms the others in damping effectiveness, as it achieves smaller amplitudes sooner. Fig. 8c indicates that placing the PVB layer in the last third closest to the hinged support leads to the greatest damping. When the viscoelastic layer is located in the middle third of the beam, vibrations dissipate by more than 99% after 2.14 seconds. For positions in the first or last thirds of the beam (positions 1 and 3), this value is 2.15 and 2.09 seconds, respectively. This suggests that placing the PVB layer in the last third of the beam contributes to improved energy dissipation for simply supported beams.

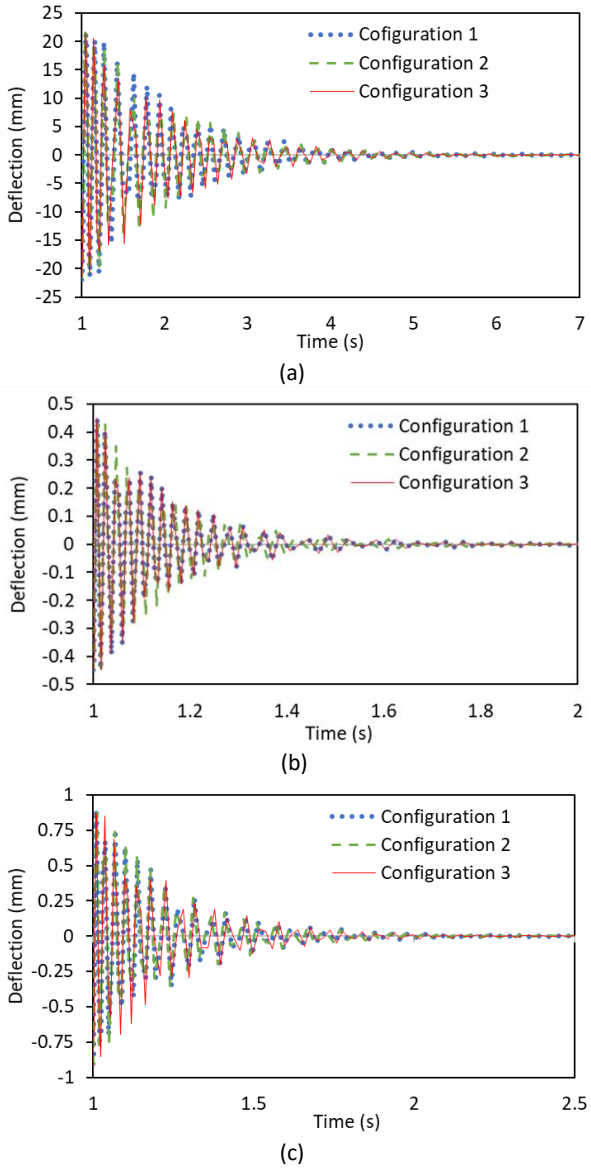

Fig. 8 Effect of axial location of the PVB layer on the time-history response of sandwich beams: (a) clamped-free, (b) clamped-clamped, (c) simply support

These results indicate that the viscoelastic layer's optimal longitudinal positioning strongly depends on the beam's boundary conditions and correlates with the regions of maximum dynamic deformation. Proper placement of the PVB layer can significantly enhance the

damping capacity and reduce the duration of vibrational responses.

4. Conclusion

This study examined the creep and dynamic behaviors of sandwich beams including viscoelastic layers using three-dimensional finite element modeling. Additionally, the study aimed to identify the optimal position of viscoelastic layers through the thickness and along the beam's length to maximize damping performance and minimize creep deformations. The accuracy of the finite element model was confirmed by comparing its results with experimental results available in the literature. The key findings of this research are summarized as follows:

- The developed three-dimensional finite element model demonstrated high accuracy in predicting both the creep behavior and the free vibration of sandwich beams incorporating viscoelastic layers.
- The inclusion of viscoelastic layers had a pronounced impact on the dynamic response of the sandwich beams, notably enhancing their damping capacity.
- Despite improving damping performance under dynamic loads, the viscoelastic layers contributed to creep behavior, resulting in increased long-term deformations under sustained service loads.
- Independent of the sandwich beam's boundary conditions, placing the viscoelastic layer near the neutral axis (i.e., at the mid-thickness) maximizes the damping effect.
- Positioning viscoelastic layers far from the neutral axis of the beam (i.e., at the top and bottom of the host beam) minimizes long-term creep deformations, irrespective of the boundary conditions.
- For clamped-free sandwich beams, placing the viscoelastic layer in the last third of the beam's length (near the free end) provides the highest damping performance. For simply supported beams, placing the PVB layer in the last third closest to the hinged support leads to improved energy dissipation. In contrast, for the clamped-clamped boundary condition, the optimal damping is achieved when the viscoelastic layer is positioned in the central third of the beam.

References

[1] Harvey Thomas Banks, Shuhua Hu, Zackary R. Kenz, "A Brief Review of Elasticity and Viscoelasticity for Solids", Advances in Applied Mathematics and Mechanics 3(1) (2011): 1-51. https://doi.org/10.4208/aamm.10-m1030

[2] Roderic S Lakes, Viscoelastic solids (1998), CRC press2017.

[3] Laura Galuppi, Gianni Royer-Carfagni, "Laminated beams with viscoelastic interlayer", International Journal of Solids and Structures 49(18) (2012): 2637-2645. https://doi.org/10.1016/j.ijsolstr.2012.05.028

[4] Fessal Kpeky, et al., "Modeling of viscoelastic sandwich beams using solid–shell finite elements", Composite Structures 133 (2015): 105-116. https://doi.org/10.13140/RG.2.1.4092.6565

[5] Nader Mohammadi, Mehrdad Nasirshoaibi, "Simulation of viscoelastic materials by ABAQUS", Mathematical Models in Engineering 1(2) (2015): 67-71.

[6] F. Pelayo, et al., "Study of the time-temperature-dependent behaviour of PVB: Application to laminated glass elements", Thin-Walled Structures 119 (2017): 324-331. https://doi.org/10.1016/j.tws.2017.06.030

[7] Maurizio Froli, Leonardo Lani, "Adhesion, Creep and relaxation Properties of PVB in Laminated Safety Glass", Glass performance days (2011): 218-21.

[8] Christian Ehrich, et al., "Development of a Novel Technique for Mechanical Characterization of Polymer Encapsulates in Laminated Glass Beams", 26th European Photovoltaic Solar Energy Conference and Exhibition, Hamburg, Germany, 2011.

[9] Tomáš Hána, et al., "Experimental and Numerical Study of Viscoelastic Properties of Polymeric Interlayers Used for Laminated Glass: Determination of Material Parameters", Materials 12(14) (2019): 2241. https://doi.org/10.3390/ma12142241

[10] Tomáš Hána, et al., "Four-Point Bending Tests of Double Laminated Glass Panels with EVA Interlayer in Various Loading Rates", Engineering Mechanics (2019): 145-148. https://doi.org/10.21495/71-0-145

[11] Alena Zemanová, et al., "On modal analysis of laminated glass: Usability of simplified methods and Enhanced Effective Thickness", Composites Part B: Engineering 151 (2018): 92-105. https://doi.org/10.1016/j.compositesb.2018.05.032

[12] Y. X. Li, et al., "State-space method for dynamic responses of double beams with general viscoelastic interlayer", Composite Structures 268 (2021): 113979. https://doi.org/10.1016/j.compstruct.2021.113979

[13] Miriam Schuster, et al., "Quantification of the linear viscoelastic behavior of multilayer polymer interlayers for laminated glass", Glass Structures & Engineering 8(4) (2023): 457-469. https://doi.org/10.1007/s40940-023-00229-w